

Ground-state structure and dynamics in a toy model for granular compaction

J.M. Luck

*Service de Physique Théorique, CEA Saclay, 91191 Gif-sur-Yvette cedex, France*¹

Abstract

We report on a toy model for the glassy compaction dynamics of granular systems, introduced and investigated in collaboration with Anita Mehta and Peter Stadler. A stochastic dynamics is defined on a column of grains. Grains are anisotropic and possess a discrete orientational degree of freedom. Gravity induces long-range directional interactions down the column. The key control parameter of the model, ε , is a representation of granular shape. Rational and irrational values of ε correspond to very different kinds of behavior, both in statics (structure of ground states) and in low-temperature dynamics (retrieval of ground states).

Key words: stochastic processes, granular media, complex systems, glassy dynamics

PACS: 02.50.Ey, 05.40.-a, 45.70.-n, 61.44.Fw

1 Foreword

In this contribution I have chosen to report on a series of works done in recent years in collaboration with Anita Mehta and Peter Stadler [1,2,3,4], where we have introduced and investigated in detail a columnar *toy model* for the compaction dynamics of granular systems in the glassy regime. The main focus of this review is on the properties of this model which are of interest in the broader context of non-equilibrium dynamics and complex systems. We emphasize the relationship between statics (structure of ground states) and low-temperature dynamics (retrieval of these ground states). Surprisingly enough, some of the key features of this model belong to Serge Aubry's favorites, such as *quasiperiodicity* and *hierarchical melting*.

Email address: luck@sph.t.saclay.cea.fr (J.M. Luck).

¹ URA 2306 of CNRS

2 Definition of the model

A columnar model for the compaction dynamics of granular media in the glassy regime has been elaborated and investigated in a series of works [1,2,3,4]. The model consists in a column of N sites, each site being occupied by a grain. Grains are assumed to be anisotropic in shape. They take, for simplicity, two possible orientations, referred to as *ordered* and *disordered*. Sites are labeled by their depth $n = 1, \dots, N$, measured from the top of the column. Orientation variables are defined by setting $\sigma_n = +1$ if grain number n is ordered, and $\sigma_n = -1$ if grain number n is disordered. A configuration of the system is thus defined by the N orientation variables $\{\sigma_n\}$.

The collective dynamics of the orientation variables is chosen in order to model the compaction dynamics of granular systems under the influence of a small vibration intensity. The crucial effect of gravity is taken into account by considering directional long-range interactions. Grain number n feels the effective weight of the whole piece of column above it ($m = 1, \dots, n - 1$). As a consequence, the upper grain (m) influences the dynamics of the lower one (n), whereas the lower grain has no influence on the dynamics of the upper one. In other words, causality acts both in space and in time. Hence there are no finite-size effects: a finite system made of N grains behaves exactly as the N upper grains of a larger (finite or infinite) system.

More specifically, we consider a Markovian stochastic dynamics defined by the following transition rates per unit time:

$$\begin{cases} w(\sigma_n = +1 \rightarrow \sigma_n = -1) = \exp\left(-\frac{\lambda_n + h_n}{T}\right), \\ w(\sigma_n = -1 \rightarrow \sigma_n = +1) = \exp\left(-\frac{\lambda_n - h_n}{T}\right), \end{cases} \quad (2.1)$$

where T is a dimensionless measure of the vibration intensity, referred to as temperature, whereas the effective activation energy λ_n and the effective ordering field h_n represent the effect of all the grains above grain number n .

In the most general model, λ_n and h_n depend on all the orientation variables σ_m for $m = 1, \dots, n - 1$. The simplest non-trivial model corresponds to [3,4]

$$\lambda_n = A n, \quad h_n = \varepsilon m_n^- - m_n^+, \quad (2.2)$$

where m_n^+ (resp. m_n^-) is the number of ordered (resp. disordered) grains above

grain number n :

$$m_n^+ = \frac{1}{2} \sum_{k=1}^{n-1} (1 + \sigma_k), \quad m_n^- = \frac{1}{2} \sum_{k=1}^{n-1} (1 - \sigma_k), \quad (2.3)$$

so that $m_n^+ + m_n^- = n - 1$.

The shape parameter ε is the essential control parameter of the model. It has to obey $\varepsilon > 0$ in order for the model to be non-trivial. It will be identified with the slope involved in the geometrical construction given below. Rational and irrational values of ε , respectively corresponding to regular and irregular grain shapes, turn out to correspond to very different kinds of static and dynamical behavior.

The amplitude A of the effective activation energy gives rise to a dynamical length

$$\xi_{\text{dyn}} = \frac{T}{A}, \quad (2.4)$$

such that the Arrhenius factor of the rates at depth n reads

$$\omega_n = \exp\left(-\frac{\lambda_n}{T}\right) = \exp\left(-\frac{n}{\xi_{\text{dyn}}}\right). \quad (2.5)$$

3 Ground-state structure

As the dynamical rules of the model are fully directional, they cannot obey detailed balance with respect to any Hamiltonian.

There is, however, a well-defined concept of *ground state*. In the zero-temperature limit we have indeed

$$\frac{w(\sigma_n = -1 \rightarrow \sigma_n = +1)}{w(\sigma_n = +1 \rightarrow \sigma_n = -1)} = \exp\left(\frac{2h_n}{T}\right) \rightarrow \begin{cases} \infty & \text{if } h_n > 0, \\ 0 & \text{if } h_n < 0. \end{cases} \quad (3.1)$$

We are therefore led to define a ground state of the system as a configuration where the orientation of every grain is aligned along its local field:

$$\sigma_n = \text{sign } h_n = \begin{cases} +1 & \text{if } h_n > 0, \\ -1 & \text{if } h_n < 0 \end{cases} \quad (3.2)$$

Table 1

Recursive construction of ground states by means of (3.2).

h_n	σ_n	$m_{n+1}^+ - m_n^+$	$m_{n+1}^- - m_n^-$	$h_{n+1} - h_n$
> 0	+1	1	0	-1
< 0	-1	0	1	ε
$= 0$?	?	?	?

(provided $h_n \neq 0$). The condition (3.2) leaves the uppermost orientation σ_1 unspecified, as h_1 vanishes identically. In the following, we assume for definiteness that the uppermost grain is ordered:

$$\sigma_1 = +1. \quad (3.3)$$

Ground states can be built in a recursive way (see Table 1). The number and the nature of ground states depend on whether ε is irrational (only σ_1 is unspecified) or rational (infinitely many orientations are unspecified). These two situations will be considered successively.

3.1 Irrational ε : Unique quasiperiodic ground state

For irrational ε , all the local fields h_n are non-zero. Table 1 implies that they lie in the bounded interval

$$-1 \leq h_n \leq \varepsilon. \quad (3.4)$$

Let us introduce the following *superspace formalism*. Consider the integers (m_n^-, m_n^+) as the co-ordinates of points on a square lattice. We thus obtain a staircase-shaped line joining the points $(m_1^-, m_1^+) = (0, 0)$, $(m_2^-, m_2^+) = (0, 1)$, etc. Vertical steps correspond to ordered grains, whereas horizontal steps correspond to disordered grains. Equation (3.4) defines an oblique strip with *slope* ε in the (m^-, m^+) plane, which contains the entire line thus constructed (see Figure 1).

A unique infinite ground-state configuration of grain orientations is thus generated. This configuration is *quasiperiodic*. The above construction is indeed equivalent to the cut-and-project method of generating quasiperiodic tilings of the line. This approach, introduced by de Bruijn in the mathematical literature [5], became then very popular in the context of quasicrystals [6].

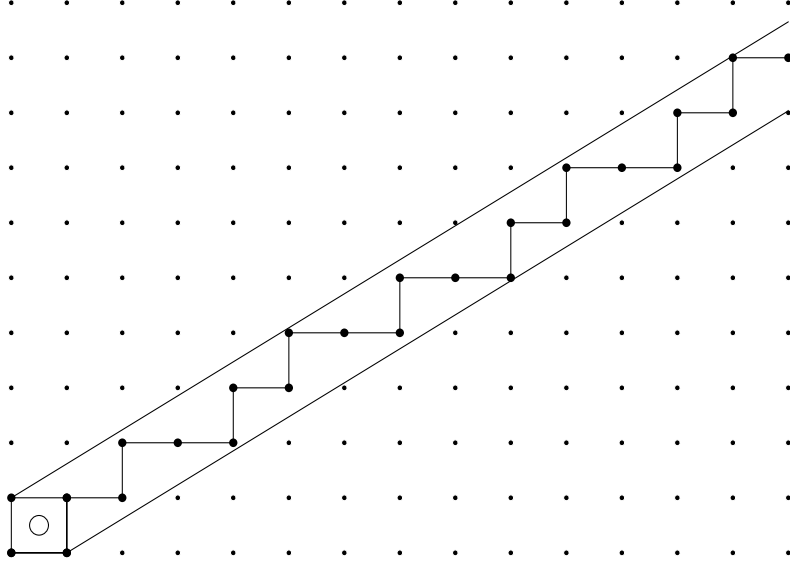


Fig. 1. Geometrical construction of the quasiperiodic ground state of the model for the golden-mean slope (3.9). The two ways of going around the first cell, marked with a circle, correspond to the two possible choices for the orientation of the uppermost grain (after [4]).

The ground state thus constructed can alternatively be described in analytical terms. We have indeed

$$m_n^+ = n - 1 - m_n^- = 1 + \text{Int}((n - 1)\Omega), \quad h_n = g(n\Omega), \quad (3.5)$$

where the *rotation number* Ω reads

$$\Omega = \frac{\varepsilon}{1 + \varepsilon} \quad (3.6)$$

and the *hull function* $g(x)$ is a 1-periodic discontinuous sawtooth function:

$$g(x) = -1 + \frac{\text{Frac}(x - \Omega)}{1 - \Omega}. \quad (3.7)$$

In these formulas $\text{Int}(x)$, the integer part of a real number x , is the largest integer less than or equal to x , whereas $\text{Frac}(x) = x - \text{Int}(x)$ is the fractional part of x ($0 \leq \text{Frac}(x) < 1$).

There are well-defined proportions of ordered and disordered grains in the ground state:

$$f_+ = \Omega = \frac{\varepsilon}{1 + \varepsilon}, \quad f_- = 1 - \Omega = \frac{1}{1 + \varepsilon}. \quad (3.8)$$

This geometrical construction is illustrated in Figure 1 for the most familiar of all irrational numbers [7], the inverse golden mean:

$$\varepsilon = \Phi - 1 = \frac{1}{\Phi}, \quad \Omega = 2 - \Phi = \frac{1}{\Phi^2}, \quad \Phi = \frac{\sqrt{5} + 1}{2} \approx 1.618033. \quad (3.9)$$

The corresponding configuration is given by a Fibonacci sequence [5,6,7]:

$$\{\sigma_n\} = + - - + - - + - + - - + - - + - + - - + - + - - \dots$$

3.2 Rational ε : Degenerate ground states

For a rational slope

$$\varepsilon = \frac{p}{q}, \quad \text{i.e.,} \quad \Omega = \frac{p}{p+q}, \quad (3.10)$$

in irreducible forms (p and q are mutual primes), some of the local fields h_n generated by Table 1 vanish. The corresponding grain orientations σ_n remain unspecified.

This feature of rational slopes is clearly visible on the geometrical construction. Figure 2, corresponding to $\varepsilon = 2/3$, shows that some of the lattice cells, marked with circles, are entirely contained in the closed strip (3.4). Consider one such cell. The broken line enters the cell at its lower left corner and exits the cell at its upper right corner. It can go either counterclockwise, via the lower right corner, giving $\sigma_{n+1} = -1$, $\sigma_{n+2} = +1$, or clockwise, via the upper left corner, giving $\sigma_{n+1} = +1$, $\sigma_{n+2} = -1$. Each marked cell thus generates a binary choice in the construction. This orientational indeterminacy occurs at points such that n is a multiple of the *period* $p + q$, equal to the denominator of the rotation number Ω .

The model therefore has a non-zero ground-state entropy (zero-temperature configurational entropy, complexity [8])

$$\Sigma = \frac{\ln 2}{p+q} \quad (3.11)$$

per grain. Each ground state is a random sequence of two well-defined patterns of length $p + q$, each of them made of p ordered and q disordered ones, so that (3.8) still holds for each of the ground states. The patterns only differ by their first two orientations. The first cases are listed in Table 2.

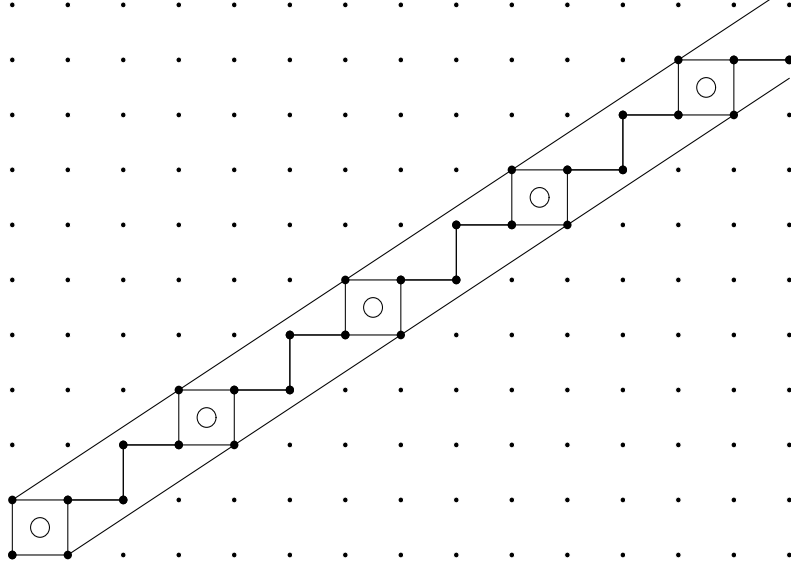


Fig. 2. Geometrical construction of the ground states of the model for the rational slope $\varepsilon = 2/3$. The marked cells, entirely contained in the strip, are responsible for the non-zero configurational entropy (after [4]).

Table 2

Patterns building up the random ground states for the first rational values of ε . The second example with period $p + q = 5$ is illustrated in Figure 2 (after [4]).

$p + q$	Ω	ε	p	q	pattern 1	pattern 2
2	1/2	1	1	1	+ -	- +
3	1/3	1/2	1	2	+ - -	- + -
3	2/3	2	2	1	+ - +	- + +
4	1/4	1/3	1	3	+ - - -	- + - -
4	3/4	3	3	1	+ - + +	- + + +
5	1/5	1/4	1	4	+ - - - -	- + - - -
5	2/5	2/3	2	3	+ - - + -	- + - + -
5	3/5	3/2	3	2	+ - + - +	- + + - +
5	4/5	4	4	1	+ - + + +	- + + + +
6	1/6	1/5	1	5	+ - - - - -	- + - - - -
6	5/6	5	5	1	+ - + + + +	- + + + + +

4 Zero-temperature dynamics. Retrieval of ground states

We have already anticipated in the previous section that the stochastic dynamics of the model simplifies in the zero-temperature limit. Equation (3.1)

indeed becomes the deterministic rule

$$\sigma_n \rightarrow \text{sign } h_n \tag{4.1}$$

(again provided $h_n \neq 0$).

The dynamical length ξ_{dyn} introduced in (2.4) is assumed to have a non-trivial zero-temperature limit. Most of the interesting features of the model are already present in the limiting case where $\xi_{\text{dyn}} = \infty$.

4.1 Irrational ε , infinite ξ_{dyn} : *Ballistic coarsening*

For irrational ε , the rule (4.1) is always well-defined, as the local fields h_n never vanish. We assume that the system is initially in a disordered state, where each grain is oriented at random: $\sigma_n = \pm$ with equal probabilities, except for the uppermost one, which is fixed according to (3.3).

Consider first the limiting situation where ξ_{dyn} is infinite. The zero-temperature dynamics is observed to drive the system to its quasiperiodic ground state. This ordering propagates down the system from its top, via *ballistic coarsening*. At time t , the grain orientations have converged to their ground-state values, given by the above geometrical construction, in an upper layer whose depth is observed to grow linearly with time:

$$L(t) \approx Vt, \tag{4.2}$$

whereas the rest of the system is still disordered. This phenomenon is similar to phase ordering, as order propagates over a macroscopic length $L(t)$ which grows forever. It is however different from usual coarsening, as the depth of the ordered region grows ballistically, with a well-defined ε -dependent ordering velocity $V(\varepsilon)$, instead of diffusively, or even more slowly [9].

The ordering velocity obeys the symmetry property $V(\varepsilon) = V(1/\varepsilon)$. Besides this property, its ε -dependence can only be investigated numerically. The ordering velocity is observed to vary smoothly with ε (although it is only defined for irrational ε), and to diverge as $V(\varepsilon) \sim 1/\varepsilon$ as $\varepsilon \rightarrow 0$. Figure 3 shows a plot of the inverse ordering velocity against ε , for $0 < \varepsilon < 1$.

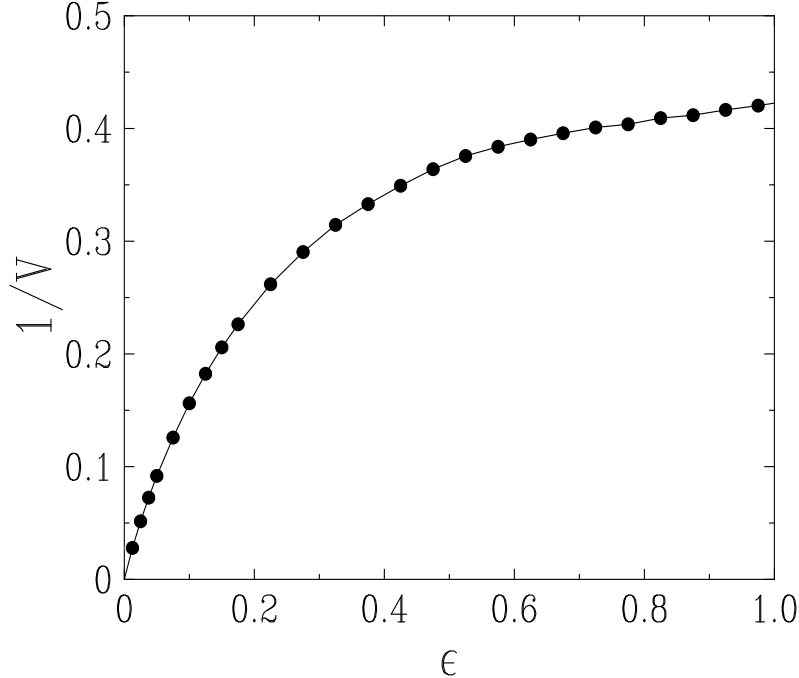


Fig. 3. Plot of the inverse ordering velocity $1/V$ of zero-temperature coarsening dynamics at infinite ξ_{dyn} , against the irrational slope ε , for $0 < \varepsilon < 1$.

4.2 Irrational ε , finite ξ_{dyn} : Crossover to logarithmic coarsening

In the general situation where ξ_{dyn} is finite, but large at the microscopic scale of a grain, the ballistic coarsening law (4.2) is modified in a minimal way, by taking into account the dependence of the rate (2.5) on depth: $dL/dt \approx V \exp(-L/\xi_{\text{dyn}})$. We thus obtain

$$L(t) \approx \xi_{\text{dyn}} \ln \left(1 + \frac{Vt}{\xi_{\text{dyn}}} \right). \quad (4.3)$$

This result exhibits a crossover between the ballistic law (4.2) for $Vt \ll \xi_{\text{dyn}}$ and the logarithmic coarsening law

$$L(t) \approx \xi_{\text{dyn}} \ln t \quad (4.4)$$

for $Vt \gg \xi_{\text{dyn}}$.

Equation (4.3) has been checked against the results of numerical simulations, for the golden-mean slope. Figure 4 shows a scaling plot of $L(t)$ corresponding to $\xi_{\text{dyn}} = 50$ and 100 , together with the prediction (4.3), with no adjustable parameter. The ordering velocity $V \approx 2.58$ is taken from the data of Figure 3.

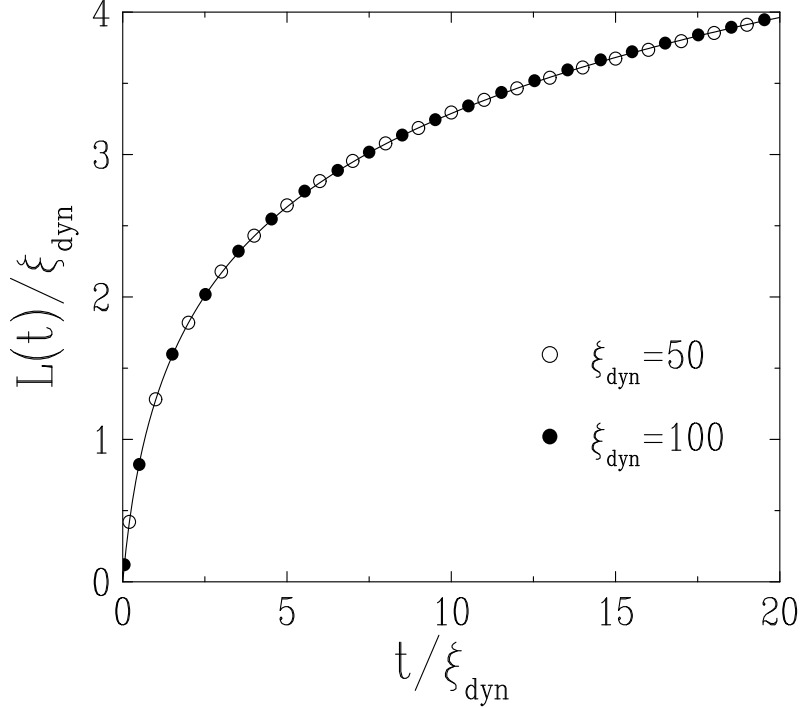


Fig. 4. Scaling plot of $L(t)/\xi_{\text{dyn}}$ against t/ξ_{dyn} for zero-temperature coarsening dynamics with the golden-mean slope. Symbols: numerical data. Full line: prediction (4.3), with $V = 2.58$.

4.3 Rational ε : Fluctuating steady state with anomalous roughening

We now turn to zero-temperature dynamics for rational ε . The updating rule (4.1) is not always well-defined, as the local fields h_n may now vanish. In such a circumstance, it is natural to choose the corresponding orientation at random:

$$\sigma_n \rightarrow \begin{cases} +1 & \text{if } h_n > 0, \\ \pm 1 \text{ with prob. } 1/2 & \text{if } h_n = 0, \\ -1 & \text{if } h_n < 0. \end{cases} \quad (4.5)$$

The zero-temperature dynamics defined in this way therefore keeps a stochastic component.

For concreteness, let us focus our attention onto the limiting situation where ξ_{dyn} is infinite, and onto the simplest rational case, i.e., $\varepsilon = 1$. Equation (2.2) for the local fields reads

$$h_n = - \sum_{m=1}^{n-1} \sigma_m. \quad (4.6)$$

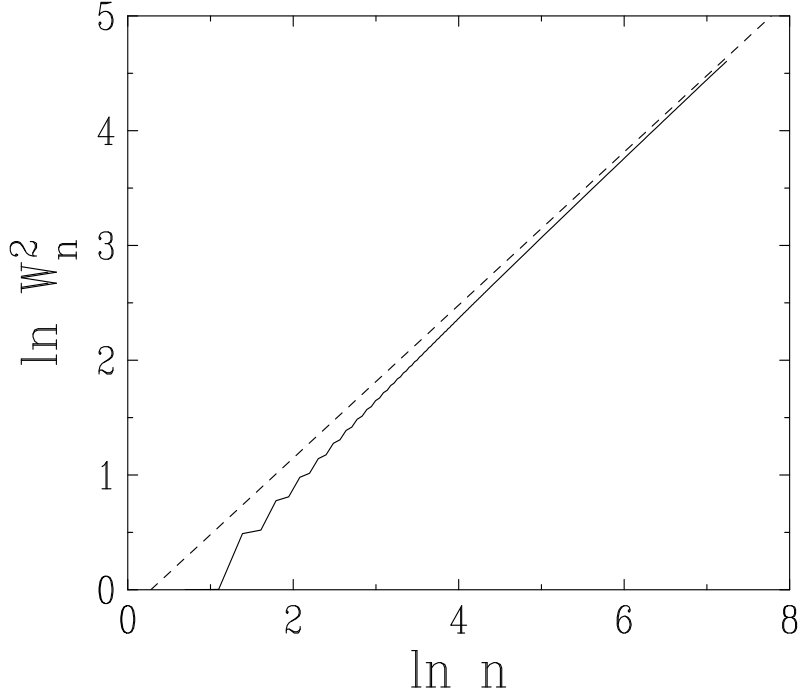


Fig. 5. Log-log plot of the local field variance $W_n^2 = \langle h_n^2 \rangle$ against depth n , for zero-temperature dynamics with $\varepsilon = 1$. Full line: numerical data. Dashed line: fit to asymptotic behavior, leading to (4.7) with $A \approx 0.83$ (after [3]).

It turns out that the zero-temperature dynamics is not able to retrieve any of the degenerate ground states. The system rather reaches a non-trivial *fluctuating non-equilibrium steady state*. This steady state is unique, i.e., independent of the initial configuration of the system. It is reached after a microscopic time.

This steady state is characterized by unbounded, albeit subextensive fluctuations of the local fields. Figure 5 indeed demonstrates that the local field variance grows as

$$W_n^2 = \langle h_n^2 \rangle \approx A n^{2/3}. \quad (4.7)$$

The exponent $2/3$ of this *anomalous roughening* law can be predicted by the following line of reasoning. Viewing the depth n as time, and the local field h_n as the position of a fictitious random walker, the noise in this walk originates in the earlier times m such that $h_m = 0$. The probability for h_m to vanish is of the order of $1/W_m$. The effective diffusion coefficient at time n therefore scales as $D_n \sim (1/n) \sum_{m=1}^{n-1} 1/W_m \sim 1/W_n$, hence $W_n^2 \sim n D_n \sim n/W_n$, i.e., $W_n^2 \sim n^{2/3}$.

Another way of characterizing this fluctuating steady state consists in looking at the probabilities $p(\mathcal{C})$ of all the microscopic configurations \mathcal{C} . Figure 6 shows a plot of the normalized probabilities $2^{12} p(\mathcal{C})$, against the $2^{12} = 4096$

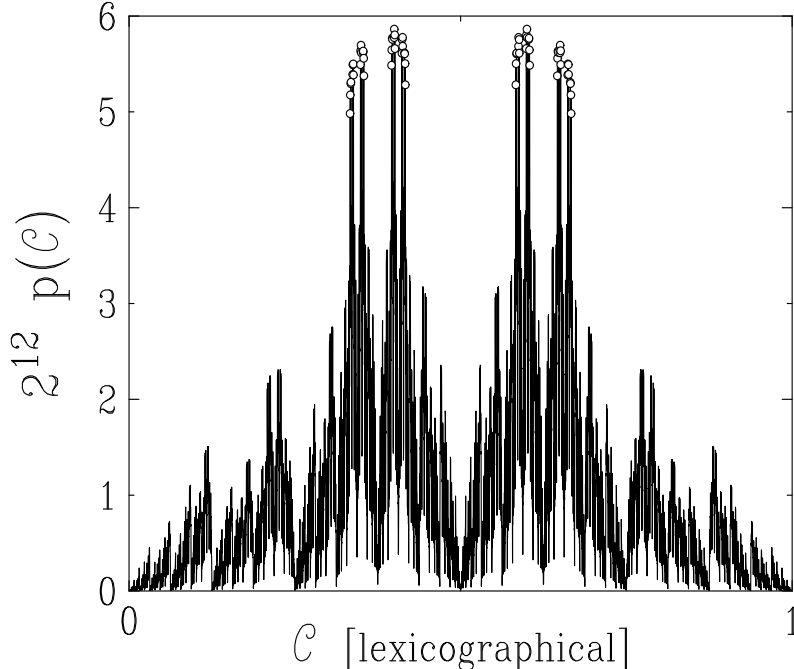


Fig. 6. Plot of the normalized probabilities $2^{12} p(\mathcal{C})$ of the configurations of a column of 12 grains in the zero-temperature steady state with $\varepsilon = 1$, against the configurations \mathcal{C} in lexicographical order. Open circles: degenerate ground states (after [4]).

configurations \mathcal{C} of a column of 12 grains for $\varepsilon = 1$, sorted according to lexicographical order (read down the column). This plot exhibits a rugged and seemingly fractal structure with self-similarity at all scales. The most frequently visited configurations are the $2^6 = 64$ degenerate ground states of the system, shown as open circles.

The knowledge of all the steady-state probabilities $p(\mathcal{C})$ gives access to the entropy of the fluctuating steady state, defined by means of the Boltzmann formula

$$S = - \sum_{\mathcal{C}} p(\mathcal{C}) \ln p(\mathcal{C}). \quad (4.8)$$

An estimate for the entropy S can be derived by using the main feature of the zero-temperature steady state, i.e., the roughening law (4.7). Think again of the depth n as a fictitious discrete time, and of the local field h_n as the position of a random walker at time n . For a free lattice random walk of n steps, one has $\langle h_n^2 \rangle = n$, and the entropy reads $S_{\text{flat}} = n \ln 2$, as all configurations are equally probable. In the present situation, the entropy S is reduced with respect to S_{flat} , because $\langle h_n^2 \rangle = W_n^2 \ll n$. The entropy reduction can be estimated as $\Delta S = S_{\text{flat}} - S \sim \sum_{m=1}^n 1/W_m^2 \sim n^{1/3}$. Figure 7 shows a plot of the entropy reduction ΔS against n . A reasonable agreement with the above estimate is

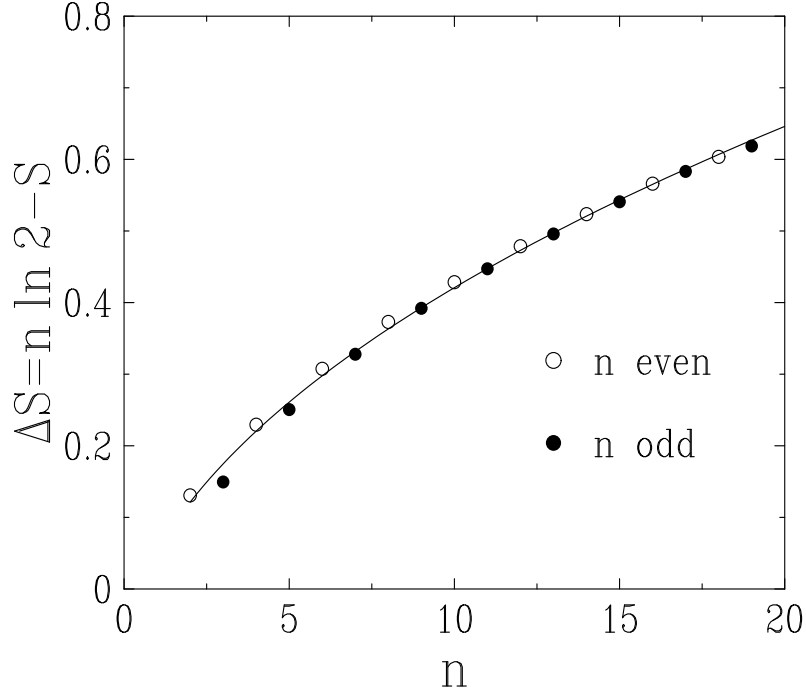


Fig. 7. Plot of the entropy reduction $\Delta S = S_{\text{flat}} - S$ in the zero-temperature steady state with $\varepsilon = 1$, against depth n . Symbols: numerical data. Full line: fit $\Delta S = (62 \ln n + 53)10^{-3} n^{1/3}$ (after [4]).

found.

The total entropy S of the fluctuating steady state is therefore equal to $S_{\text{flat}} = n \ln 2$, up to a small subextensive reduction ΔS of order $n^{1/3}$. The equality of the extensive part of S with S_{flat} can be viewed as a manifestation of the flatness hypothesis of Edwards [10].

5 Low-temperature dynamics

We now turn to the investigation of the dynamics of the model for a low but non-zero temperature T . We consider for simplicity the case of an infinite ξ_{dyn} .

If the slope ε is rational, the rule (4.5) is already stochastic at zero temperature, so that no qualitatively novel effect appears at low temperature.

We therefore focus our attention onto the case of an irrational slope ε . We recall that the zero-temperature dynamics (4.1) drives the system to its quasiperiodic ground state, where each orientation is aligned with its local field, according to (3.2). For a low but non-zero temperature T , there will be *mistakes*, i.e., orientations $\sigma_n = -\text{sign } h_n$ not aligned with their local field. Equation (3.1)

suggests that the probability of observing a mistake at site n scales as

$$\Pi(n) \sim \exp\left(-\frac{2|h_n|}{T}\right). \quad (5.1)$$

Hence the most fragile sites n , such that the local field h_n is relatively small in the ground state ($|h_n| \sim T \ll 1$), will be preferred nucleation sites for mistakes, and thus govern the low-temperature dynamics.

These nucleation sites can be located as follows. Equation (3.5) shows that the local field h_n is small when $n\Omega$ is close to an integer m . The latter turns out to be $m = m_n^+$. Indeed

$$n\Omega = m + \delta \implies h_n = \frac{\delta}{1 - \Omega}, \quad (\Omega - 1 < \delta < \Omega). \quad (5.2)$$

The most active nucleation sites are therefore in correspondence with rational numbers m/n which are the closest to the irrational rotation number Ω . Finding these rational approximants is a well-defined problem of Number Theory, referred to as Diophantine approximation [7].

Let us illustrate this on the example of the golden-mean slope (3.9). We are led to introduce the Fibonacci numbers F_k [6,7], defined by the recursion formula

$$F_k = F_{k-1} + F_{k-2} \quad (F_0 = 0, \quad F_1 = 1). \quad (5.3)$$

We have alternatively

$$F_k = \frac{\Phi^k - (-\Phi)^{-k}}{\sqrt{5}}. \quad (5.4)$$

The leading nucleation sites are the Fibonacci sites $n = F_k$. We have $m = m_n^+ = F_{k-2}$, $m_n^- = F_{k-1}$, and $h_n = (-)^k \Phi^{-(k-1)}$, so that

$$\Pi_k = \Pi(F_k) \sim \exp\left(-\frac{2\Phi}{\sqrt{5}TF_k}\right). \quad (5.5)$$

We can therefore draw the following picture of low-temperature dynamics. Mistakes are nucleated at the Fibonacci sites F_k , according to a Poisson process, with exponentially small rates proportional to the Π_k . They are then advected with constant velocity $V \approx 2.58$, just as in the zero-temperature case. The system is ordered according to its quasiperiodic ground state in an upper layer ($n < \mathcal{N}(t)$), while the rest is disordered, somehow like the zero-temperature steady state for a rational slope. The depth $\mathcal{N}(t)$ of the ordered

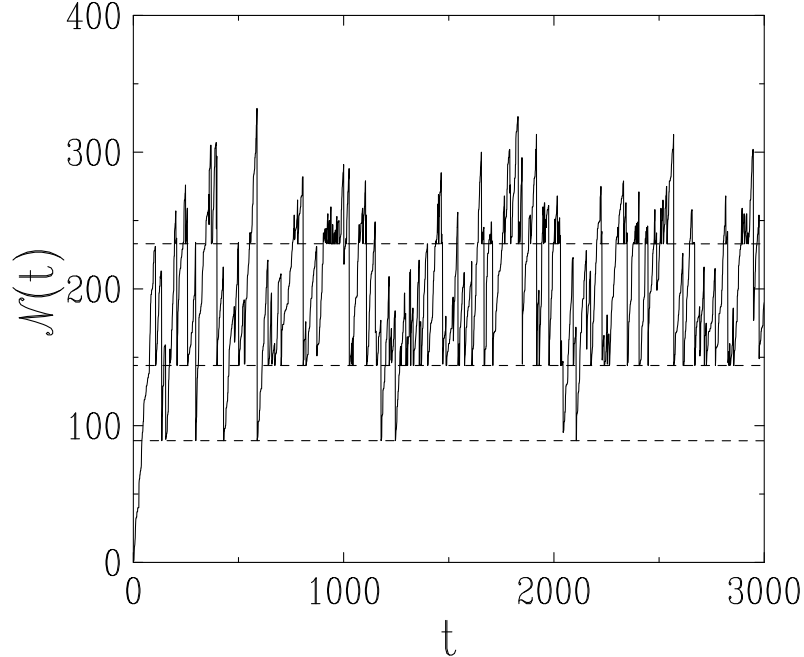


Fig. 8. Plot of the instantaneous depth $\mathcal{N}(t)$ of the ordered layer against time t , for the golden-mean slope, and temperature $T = 0.003$. Dashed lines: leading nucleation sites given by consecutive Fibonacci numbers (bottom to top: $F_{11} = 89$, $F_{12} = 144$, $F_{13} = 233$) (after [3]).

layer, given by the position of the uppermost mistake, is therefore a natural collective co-ordinate describing low-temperature dynamics.

Figure 8 shows a typical sawtooth plot of the instantaneous depth $\mathcal{N}(t)$, for a temperature $T = 0.003$. The leading nucleation sites are observed to be given by Fibonacci numbers.

The system thus reaches a steady state, characterized by a finite ordering length $\langle \mathcal{N} \rangle$, which diverges at low temperature, as mistakes become more and more rare. The law of this divergence can be predicted by the following argument. The most active nucleation Fibonacci site is such that the nucleation time $1/\Pi_k$ is comparable to the advection time to the next nucleation site F_{k+1} , i.e., $(F_{k+1} - F_k)/V \approx F_k/(\Phi V)$, hence $\Pi_k F_k \sim \Phi V$. Less deep sites have too small nucleation rates, while the mistakes nucleated at deeper sites have little chance to be the uppermost ones. Equations (5.5) then yields

$$\frac{\sqrt{5}}{2\Phi} T F_k \ln \frac{F_k}{\Phi V} \approx 1, \quad (5.6)$$

hence

$$\langle \mathcal{N} \rangle \approx F_k \approx \frac{2\Phi}{\sqrt{5}} \frac{|\ln T|}{T}. \quad (5.7)$$

The estimate (5.6) correctly predicts that $F_{12} = 144$ is the most active nucleation site at temperature $T = 0.003$ (see Figure 8).

Both the existence of a well-defined sequence of preferred nucleation sites, and the divergence of the depth of the most active nucleation site as $\langle \mathcal{N} \rangle \sim |\ln T|/T$, are very reminiscent of the phenomenon of hierarchical melting, put forward by Serge Aubry and collaborators [11]. This effect manifests itself as peaks in the specific heat at low temperature in some incommensurate modulated solids, each peak being in correspondence with a temperature-dependent spatial scale, where the system is more fragile and preferentially melts.

6 Outline

In a series of recent works [1,2,3,4] we have introduced and investigated in detail a columnar *toy model* for granular compaction. The minimal model of interest described in this report has one essential parameter, the shape parameter ε , which gives the slope of the geometrical construction of ground states within the superspace formalism.

Rational and irrational values of ε correspond to very different kinds of behavior, both in statics (structure of ground states) and in low-temperature dynamics (retrieval of these ground states).

For irrational values of ε :

- The model has a unique quasiperiodic ground state.
- Zero-temperature dynamics leads to a fast retrieval of this ground state by means of the ballistic growth of the thickness of the ordered top layer.
- A crossover to a logarithmic growth takes place when this depth becomes comparable to the dynamical length.
- Low-temperature dynamics involves the nucleation of mistakes at preferred nucleation sites. This phenomenon is analogous to hierarchical melting.

For rational values $\varepsilon = p/q$:

- The model has extensively degenerate ground states and therefore a positive configurational entropy.
- Ground states consist of random sequences of two well-defined patterns consisting of $p + q$ grains.
- Zero-temperature dynamics is not able to retrieve any of the ground states.
- The system is rather driven into a non-trivial fluctuating steady state characterized by unbounded, albeit subextensive fluctuations in the local fields.

References

- [1] P.F. Stadler, A. Mehta, and J.M. Luck, *Adv. Complex Systems* **4**, 429 (2001).
- [2] P.F. Stadler, J.M. Luck, and A. Mehta, *Europhys. Lett.* **57**, 46 (2002).
- [3] A. Mehta and J.M. Luck, *J. Phys. A* **36**, L365 (2003).
- [4] J.M. Luck and A. Mehta, *Eur. Phys. J. B* **35**, 399 (2003).
- [5] N.G. de Bruijn, *Nederl. Akad. Wetens. Proc. A* **84**, 27 (1981).
- [6] M. Duneau and A. Katz, *Phys. Rev. Lett.* **54**, 2688 (1985).
M. Duneau and A. Katz, *J. Phys. (France)* **47**, 181 (1986).
V. Elser, *Phys. Rev. B* **32**, 4892 (1985).
P.A. Kalugin, A.Yu. Kitayev, and L.S. Levitov, *JETP Lett.* **41**, 145 (1985).
P.A. Kalugin, A.Yu. Kitayev, and L.S. Levitov, *J. Phys. (France) Lett.* **46**, L601 (1985).
- [7] G.H. Hardy and E.M. Wright, *An Introduction to the Theory of Numbers* (Clarendon, Oxford, 1990).
- [8] J. Jäckle, *Phil. Mag. B* **44**, 533 (1981).
R.G. Palmer, *Adv. Phys.* **31**, 669 (1982).
- [9] A.J. Bray, *Adv. Phys.* **43**, 357 (1994).
- [10] S.F. Edwards, in *Granular Matter: An Interdisciplinary Approach*, ed. A. Mehta (Springer, New York, 1994).
- [11] F. Vallet, R. Schilling, and S. Aubry, *Europhys. Lett.* **2**, 815 (1986).
R. Schilling and S. Aubry, *J. Phys. C* **20**, 4881 (1987).
F. Vallet, R. Schilling, and S. Aubry, *J. Phys. C* **21**, 67 (1988).